Simulation of Effects of Piston Ring Parameters on Ring Movement, Friction, Blow-by and LOC

Hans H. Priebsch
Hubert M. Herbst

AVL List GmbH, Austria

MTZ

November 1999

Simulation of Effects of Piston Ring Parameters on Ring Movement, Friction, Blow-by and LOC

Hans H. Priebsch
Hubert M. Herbst

AVL List GmbH, Austria

MTZ
November 1999

Without a doubt, a number of programs for the simulation of piston ring dynamics and blow-by enables trend calculations. Nevertheless, there are only a very few that enable the calculation of absolute values for interring pressures, ring movement, and blow-by with the same set of boundary conditions. To simulate absolute values comparable with measured ones, the methodology programmed in software AVL GLIDE has been successful. A comparison with measurements and a study of ring design parameters on a truck diesel engine are presented here.

1 Introduction

To fulfill future emission regulations requires an optimization of all engine components concerned with the combustion process. Here, due to their sealing function, piston rings have a dominant influence on blow-by and lube-oil-consumption (LOC).

The classical selection of suitable rings in the design stage is based on the experience of designers and is checked in the engine tests later on. Nevertheless, the increased demands for the reduction of costs and time to market in the development of vehicle engines also requires the use of advanced simulation tools for this subject. The simulation of the ring movement should enable both, the improvement of the design and to understand and explain phenomena and errors occurring in the test of prototype engines.

Piston rings have to provide optimum sealing function, low wear and friction, all at the same time. The movement of rings is determined by the movement of the piston in the deformed liner on one hand and by the loads on the single ring (e.g. due to gas, masses, friction) on the other. The correct modeling of the physical behavior of the piston rings under running engine conditions is complex due to the interaction of completely different structures, e.g. oil, gas and elastic bodies. The concept of this methodology, described in this paper, was originally based on findings of applications of the older FVV software [1]. The physical models introduced in GLIDE exceed the former FVV ones significantly and are completed by a simulation of LOC. A short time ago, the performance was again proven in a benchmark organized by the American companies Cummins and Federal Mogul. GLIDE won this competition. The results described in this paper resulted from simulations and tests of truck engines that ranged between 1.5 and 2 liters/cylinder.

2 Model and prediction of ring dynamics and LOC

In **Figure 1,** the procedure of predicting ring dynamics and LOC is presented. In the first step, the lateral and tilting movement of the piston, which has a significant impact on ring dynamics, is determined. Thereby, the ball shaped surface of the elastic piston, which is defined by discrete nodes over piston height, makes a motion within the clearance along the rigid liner surface. The method is suitable for mono-pistons and articulated pistons.

For the design of piston rings, the sealing effect towards the crankcase, oil film distribution on the liner wall and the axial ring motion have to be analyzed. The sealing effect is achieved because the rings are pressed against the cylinder wall and against the bottom face side of the piston groove on the other by gas forces. In the direction towards the liner wall, the seating is additionally increased by the initial tension of the ring.

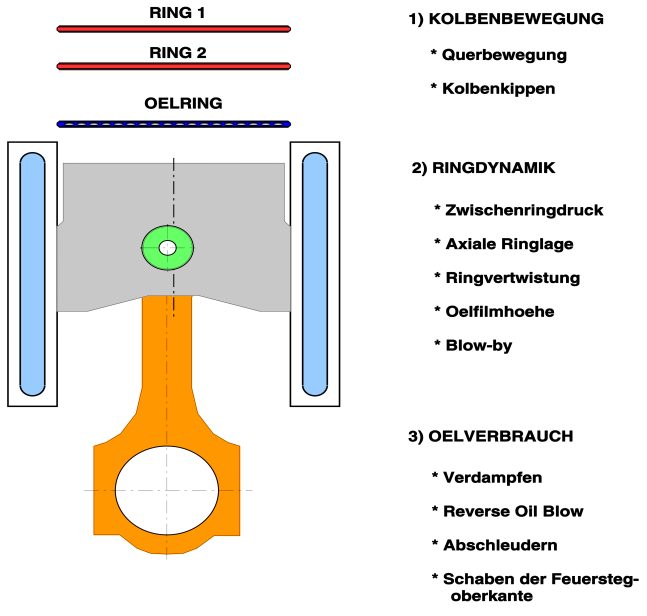

Fig. 1: Model and procedure of a GLIDE simulation

Inertia forces from the oscillating vertical movement and shear forces from the secondary movement of the piston influence this sealing effect due to the reduction in contact pressure. The results are blow-by in the direction of the crankcase and engine-power decrease. Furthermore, the penetrated combustion gas can raise the temperature in the ring pack so much, that a smooth operating of rings and piston is no longer guaranteed due to carbon deposit, wear etc.

Besides the function of sealing, the rings must ensure a sufficient lubrication of the liner wall for the subsequent upward stroke. The height of the left oil film is substantially influenced by the radial ring load, the sliding velocity, and the actual running face geometry. Further influences are oil property, local temperature, and the characteristic of the liner surface.

Controlling the ring motion in the piston groove is a requirement for a sufficiently long and smooth ring operation. The hazards are ring break due to flattering, loss of sealing, and more. Since the motion of the rings and the lubrication are substantially influenced by the gas forces, and therefore connected to the pressure in the entire ring pack, the evaluation of that is a central issue in the dynamics of piston rings.

2.1 Pressure set up in the ring pack

The mechanism of piston ring sealing is equivalent to a labyrinth seal, where the gap clearances are determined by the actual position of the rings in the groove. **Figure 2** shows the modeling of the ring pack by a system of vessels connected by orifices. In contrast to former models [1,4,5], extra orifices at the oil ring and the piston top land were added. The latter controls flow of the combustion gas towards the top ring dependent on the gap clearance. In particular, for diesel engines there is significant difference of the gaps at Anti-Thrust (ATS) and Thrust Side (TS) during the change of seating of piston at FTDC.

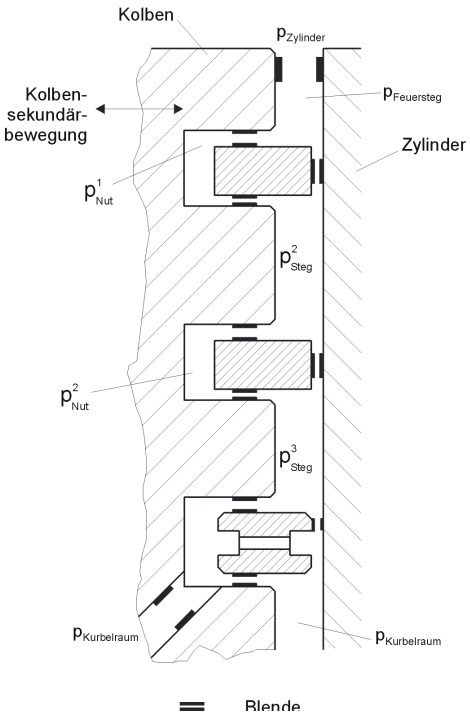

Fig. 2: Orifice model of ring pack

The pressures in the volume behind p_{Nut} and below the ring p_{Steg} are obtained by time integration from the cross flow from one into other vessel. For the calculation of the gas flows, the law for isentropic flow of ideal gas is used Equation(1). The calculation of the updated gas pressures due to changes in mass and vessel volume is described by the isothermic equation of state. This requires a steady state temperature with the surrounding Equation(2). This is taken into account by input of the particular piston temperature given by a measurement or FEM. In context with discharge coefficients, the real mass flow rate is determined from the ideal flow. This flow considers, in addition to the decrease of velocity, the contraction of the jet and the change of density due to friction.

On one hand, the areas of the orifices are determined by the axial gap between ring and groove face side. On the other hand, the areas are determined by the radial gap between piston land towards the liner wall and ring gap end clearance. Furthermore, the design features at rings and piston land-like chamfers and cut edges increase the flow area and considered according [6]. It is taken into account that rings with sealed gap ends and a seating at the bottom ring side and as well at liner wall would completely prevent any gas flow. Measurements have shown that despite good form matching capability of the rings, gas passes those contact areas. In Equation(3), rest flow areas are defined by an equivalent gap height (roughness and geometrical accuracy) dependent on the contact pressure and structural elasticity of either surfaces. It is also possible to model a uneven support in angular direction determined by pre-twisted rings with an appropriate increase of start gap width and soft contact behavior. This method ensures a large flow area at low contact forces between ring and piston groove sides. This leads to an increased gas flow at that moment. Even if the load is slightly increased in that state, the result is a relatively sharp closing of the flow passage.

2.2 Hydrodynamics of the piston rings

During the strokes of the piston, the sliding of rings is largely equivalent to the motion of an inclined floating block. At the dead-center position, the block reaches the minimum, and at medium stroke, the maximum magnitude dependent on actual velocity, shape of the gap, and filling rate. In the fired engine, the gaps are achieved. These are almost in the range of the roughness on the liner wall. In that case, the pressure set-up in the lubrication gap is significantly influenced by the roughness. The methodology presented in [7, 8] determines the influence of the roughness on the surface as well as their orientation on the pressure distribution by extending the Reynolds equation about shear and pressure terms as shown in Equation(4). The solver is described in [2]. Important is the mass balance in the entire ring pack, that is, each ring is supplied with the amount of oil which corresponds with the left oil. The result is an oil film as a function of time and position.

2.3 Lube Oil Consumption

The last section of the simulation procedure deals with the evaluation of oil loss to the combustion gas. This is determined by evaporation from the liner wall, throw off above the top ring, reverse oil blow through the gap end into the combustion chamber, and scraping of oil films at the liner wall [2]. Which kind of loss is dominant in the actual case is a matter of the particular operating condition and the outline of the lubrication. It is proven that evaporation plays a major role at high temperatures of the components, whereas the

mechanical losses at high inertia forces are dominant. The first corresponds either with an operation condition from about rated power up to full load or the second at high speed and idle. Above all, the contribution due to oil pumping at the top ring is depended by the amount of left at the oil ring. There is an idea about, that due to axial ring motion relatively towards the piston groove oil is squeezed out of the ring side faces. However, in view of the large amount of gas (that stream either in or out of the volume behind the top ring passing the ring side face during intake and power stroke), oil is lost due to evaporation rather than to pumping.

The loss of oil at the liner wall is defined by the mass transfer through the phase boundary given by the residual oil film and the combustion gas, which is either sent with the combustion gas or burned at sufficiently high temperature. The evaluation of the evaporation rate is based on the steady state connective mass transfer as described in Equation(5) and is considerably influenced by the temperature, pressure, and velocity of the combustion gas [9,10]. For defining the diffusion coefficient and the density of oil vapor layer, the oil surface temperature is needed. At each time step, the temperature in the boundary layer between oil vapor and combustion gas is determined by solving the equation of heat transfer. This equation needs the liner wall temperature as well as the temperature of the combustion gas determined by a measurement or FEM.

In the term of throw off, all losses of oil that are thrown into the combustion chamber due to inertia forces during the upward stroke of the piston are collected. The amount of thrown off oil is determined by the magnitude of the inertia force and can come to maximum amount of oil which is currently available above the top ring. For defining the available amount of oil, the flow rates are considered given by the balance of the left oil heights at the liner wall during one downward and upward stroke of the piston, as well as amounts of oil flow rates coming from the squeeze effects at the top ring. The reduction of that oil amount, which is blown down through the ring end gap at higher gas pressures in the combustion chamber than in the second piston land, leads to the mass balance according Equation(6). The evaluation of throw off is modeled by several layers according to [11], where the oil flow rate is defined by the balance of the mean velocity for steady state and mean velocity Equation(7).

The third part in losses of the total oil consumption in the range piston is defined by oil flow rates through the ring end gap at pressures where the pressure in the second piston land exceeds that of the chamber. All blown oil is immediately counted as oil loss evaluated according Equation(8).

The demand after low particle emission makes it necessary to have a very small gap clearance in between piston top land and liner wall. Additionally, the deposit on top land closes the gap and leads to the effect that the oil film is scrapped towards the combustion chamber by the deposits during the upward stroke. This loss is calculated according geometrical relations defined by the overlapping of the top land with the oil film.

3. Comparison between measurement and simulation

In order to verify the results of the simulation, a number of measurements of piston secondary movement, ring motion, inter-ring pressure and lube oil consumption have been carried out by AVL at several operating conditions. The work was carried out in co-operation with Federal-Mogul Burscheid GmbH (the former AE Goetze). These measurements have made it possible to check the model concerning its reliability and to evaluate the correction factors which formerly have been insufficiently known. The measurement was performed on a turbocharged 6-cylinder truck diesel engine with a displacement of 2 liters each cylinder. The comparison of measurement and simulation is shown in **Figure 4** as a representative for the number of measured operating conditions. The measured gas pressures over crank angle in the combustion chamber, as well as in the volumes at second and third piston land, are drawn in the diagram in the left corner. The pressures achieve a maximum magnitude of about 5 bars absolute nearby 40 degrees after FTDC. It is remarkable, that there is a substantial difference in gas pressure at TS and ATS. This is due to the fact that the secondary piston movement results in a difference of the volumes at the piston land and that different discharge areas are achieved due to inclined position of the piston. **Figure 3** shows the predicted movement by means of lateral displacement of and tilting around the piston pin. Whereas, the lateral displacement shows a typical characteristic of piston movement that the trend of the tilting turns out, how the piston inclines its crown towards TS due to the piston pin offset to ATS. If the piston movement is thought to be assigned to the changes of the volumes below the top ring, the smaller volume on ATS causes a larger pressure gradient. After FTDC, the distribution of volume is reversed due to the change of seating of the piston, which causes a higher inertia of the subsystem due to a larger amount of gas mass on ATS. This results in a delay of the pressure release contrary to TS.

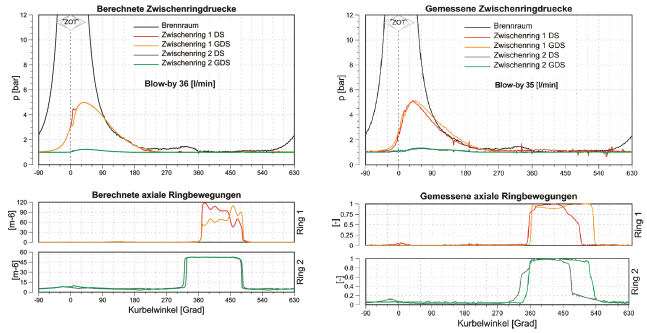

Fig. 4: Comparison of pressures and ring motions at medium load

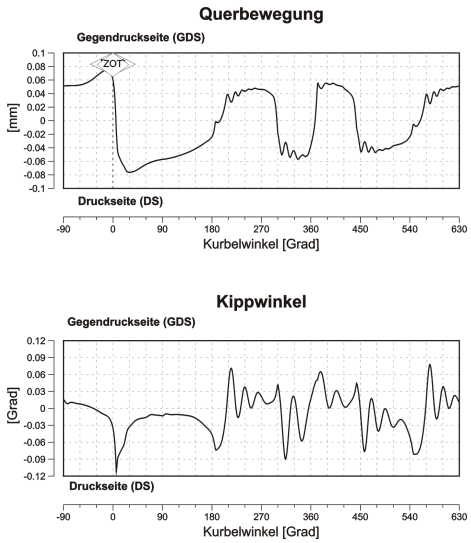

Fig. 3: Piston secondary movement at medium load

The measurement of ring axial motion shows only one change of seating over the entire cycle, respectively. Only in the range 45 degrees before FTDC does the measurement signal come up with a short lift on TS. The tip on the scale, which finally leads to a lift off and causes a substantial pressure release, could be a small disturbing like angular rotation of the ring, cyclic changes of the combustion gas pressure trend and piston secondary movement, as well as changes in the axial friction due to the oil temperature. Furthermore, it should be indicated that the convex trend of the axial motion at the top ring on TS and the concave at ATS, respectively, displays the motion of the ring relatively to the piston ring groove. Overall, a very good correlation was achieved between measurement and simulation.

4 Application and parameter study

The animation of the dynamics of piston and rings with moving images should make it easier to analyze the results and offer some details which might be not visible by the merely inspection of the diagrams. In **Figures 5** and **6**, there are sequences of the animation for piston secondary movement and ring motion. Beside the possibility of displaying the contour and motion in an enlarged scaling, the vectors of forces and pressures are also shown, respectively.

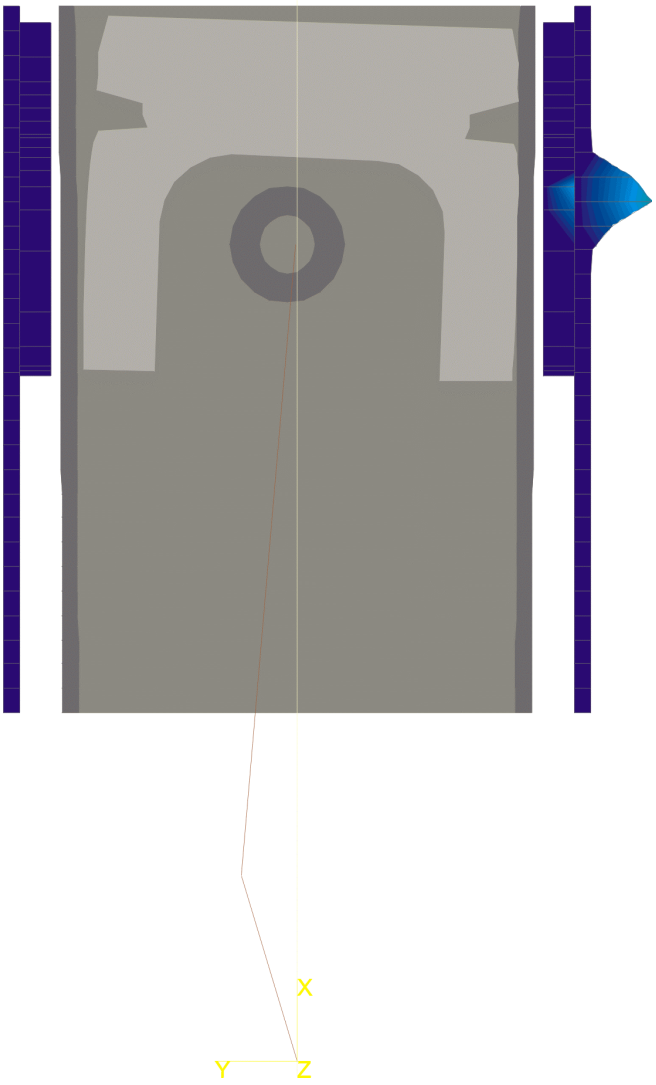

Fig. 5: Animation of piston movement in GLIDE, change of seating FTDC

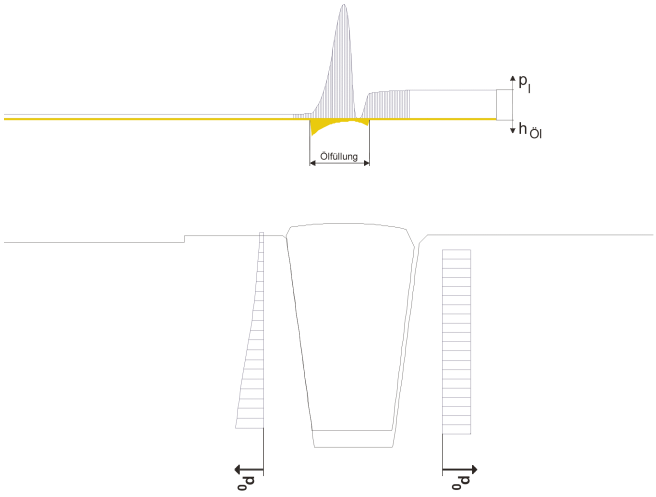

Fig. 6: Animation of piston ring motion in GLIDE, downward stroke

4.1 Influence of the pre-twist angle on the sealing at ring bottom side

Pre-twisted rings have a groove-like chamfer or rectangular cut back on the back side. This causes a plate-shaped deformation of the ring at mounting position. Taper-faced rings are often performed with such a groove on the top edge, whereby both the inclination angle between running face towards the liner wall and scrapping effect is increased. This results in positive twisting. Beside that design, there are rings that have the groove on the bottom edge and twist into opposite direction. This results in negative twist. Rings having that design achieve a lower LOC in comparison to positive twisted rings. In the current investigation the influence on gas pressure distribution at the bottom ring side face and sealing effects is currently being investigated.

In **Figure 7,** a sequence from the ring animation is shown for negative (a) and positive pre-twisted ring (b). Whereas the pressure distribution along the top ring side face does not show any remarkable differences, the one at the bottom side is exactly contrary. This is because of the different seating points at the rings. Due to the negative pre-twisting of the ring in case (a), a wedge-shaped gap is set up between ring and groove side, which defines a front edge bearing contact. The sealing effect is mainly achieved at that point which leads to a appropriate large pressure drop. As a result of the higher gas load at the ring bottom ring side face, the net-load in axial direction towards the crankcase is smaller. The characteristic of the second ring is changed in such a way that due to the smaller load, any pre-twisted ring changes their seating even at lower engine speed in the range of FTDC. Furthermore, a larger discharge area remains at the bottom ring side face. Both effects will lead to higher amount of blow-by [12].

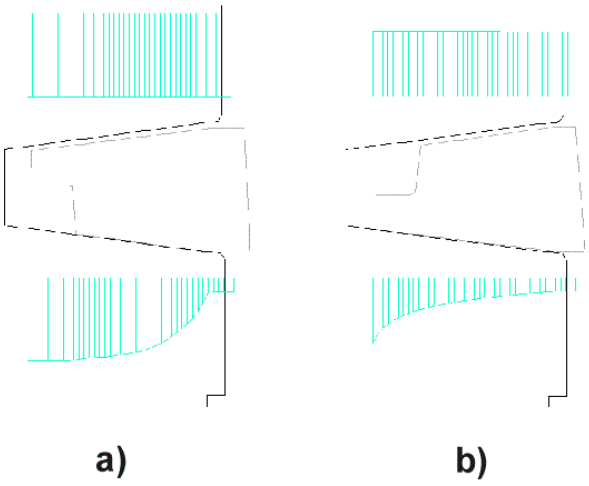

Fig. 7: Predicted gas pressure distribution at ring sides of torsion and reverse torsion rings

4.2 Influence of the tangential force at the oil ring on friction loss and LOC

Starting at the basic ring pack, two variants with doubled and half tangential force for the oil ring have been investigated by means of friction pressure loss and lube oil consumption. **Figure 8** shows the friction losses of the rings separately and the total value for the baseline as well as for variants. The bar diagram shows that any increase of friction loss is only determined by the oil ring. This result agrees with the imagine, that substantial higher friction is generated at higher pressure on the running face at the oil ring and high sliding velocities. Furthermore, the oil ring achieves higher scrapping effect which results in a smaller left oil film height on the liner wall. Consequently, the oil supply for second and top ring is lower, but does not lead to any substantial changes of the friction losses.

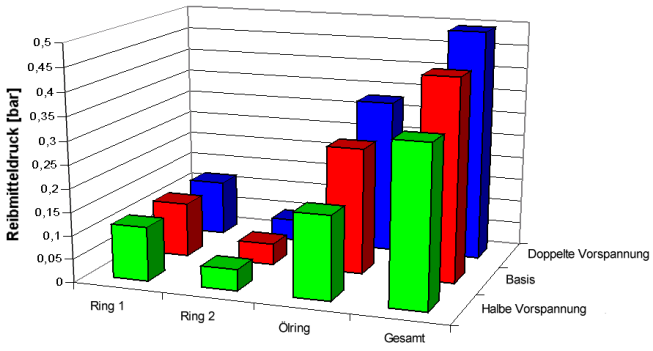

Fig. 8: Friction mean effective pressure depending on tangential force at oil ring

The simulation of LOC provides factors that allow weighting of the single LOC mechanisms. Due to this, a partial analysis of influences is possible. The partial amounts of LOC displayed in **Figure 9** refers for the baseline to following distribution: 70% evaporation, 10% oil loss due to reverse blow-by, 20% throw-off. In the current investigation any contribution on the total LOC due to scrapping at the top land is not considered. In detail, no remarkable influence of the evaporated oil amount depending from the tangential force can be stated. A definite trend is observed for those amounts given by reverse blow-by and throw off (-4% and –5%). In total a decrease of LOC of about 6% is evaluated using the ring pack with doubled tangential force. By analogy, the results using the variant with the half tangential force turn out an increase of the total LOC of about 2%.

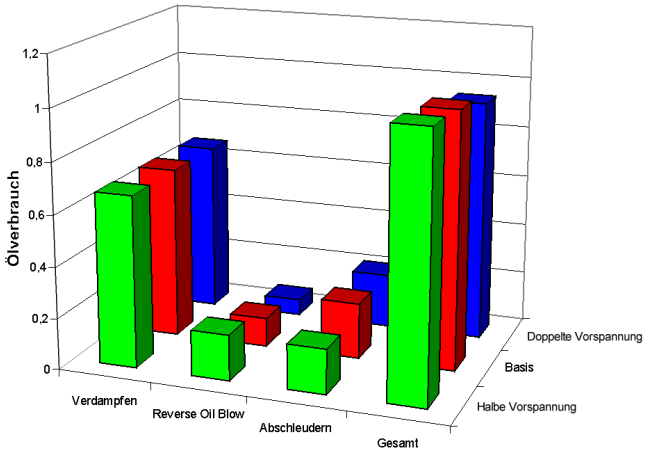

Fig. 9: LOC depending on tangential force at oil ring

5 Conclusions

From the results shown, the following conclusions can be drawn:

- Due to the methodology introduced, it is possible to calculate absolute values of ring movement, blow-by, and interring pressures despite using 2 ½ D models only, provided that geometry, filling ratio, and volumes of gas are determined properly for the given engine operating condition. This is proven by comparisons of measured and calculated results.
- Some boundary conditions (discharge coefficients, rest flow areas) need not to be tuned by experimental results for the first applications. Meanwhile, information has been established that compares measurement and calculation successively. These results can be provided for other users of GLIDE.
- The simulation results show clearly the expected increase of blow-by for negative twisted rings which can be taken as a suggestion for reduced LOC.
- Change in design parameters and their effect on friction and LOC is shown by simulation. Thus, the interaction of effects can be analyzed in the design stage and errors can be omitted earlier.

6. Equations

$$\dot{m} = A \cdot \psi \cdot p_C \cdot \sqrt{\frac{2}{R \cdot T_C}} \cdot \sqrt{\frac{\kappa}{\kappa - 1} \cdot \left[\left(\frac{p_0}{p_C} \right)^{\frac{2}{\kappa}} - \left(\frac{p_0}{p_C} \right)^{\frac{\kappa+1}{\kappa}} \right]} \qquad (1)$$

$$p_C = \frac{R \cdot T_C}{V_C} \cdot \left(m + \dot{m} \Delta t \right) \qquad (2)$$

$$A = A_0 \, e^{\frac{p_F \, f_\varepsilon}{50}} \qquad (3)$$

$$\frac{\partial}{\partial x} \left(\Phi_x h^3 \frac{\partial \bar{p}}{\partial x} \right) = 6 \eta U \frac{\partial \bar{h}_T}{\partial x} + 6 \eta U \sigma \frac{\partial \Phi_s}{\partial x} + 12 \eta \frac{\partial \bar{h}_T}{\partial t} \qquad (4)$$

$$\frac{\beta}{R_f\, T_f}(p_f - p_\infty) = -\frac{D}{R_f\, T_f}\frac{dp}{dr} = \dot{g} \tag{5}$$

$$V_{Top} = V_{\Delta h_F} + V_p - V_{St} \tag{6}$$

$$V_{Ab} = (\overline{u} - \overline{u}_{St}) h_F U_F \Delta t,\ V_{Ab} \le V_{Top} \tag{7}$$

$$V_{St} = \frac{a^2 \Delta p}{8\pi\eta B}\Delta t \tag{8}$$

A = orifice area

A_0 = orifice area unloaded

B = width of ring running face

D = diffusion coefficient

R = gas constant, air

R_f = gas constant, oil vapour

T_C = vessel temperature

T_f = oil layer temperature

U = sliding velocity

U_F = perimeter at piston top land

V_{Ab} = thrown-off oil

V_C = vessel volume

V_{St} = volume of reverse blow-by

V_{Top} = accumulated oil

V_p = pumped oil

$V_{\Delta h_F}$ = balance of volume for oil film

a = edge at gap end area

f_ε = elasticity of surface

$\dot{g}$ = mass flow rate

h = gap clearance

h_F = thickness of oil layer

$\overline{h}_T$ = average gap clearance

m = mass of gas

$\dot{m}$ = gas flow rate

p = combustion pressure

p_o = pressure of surrounding

p_C = vessel pressure

p_F = contact pressure

$\overline{p}$ = mean hydrodynamic pressure

p_f, p_∞ = oil vapour pressure

r = radial dimension

t = time

$\overline{u}, \overline{u}_{St}$ = mean in-stationary and stationary velocity of oil layer

x = dimension in sliding velocity

Δp = pressure gradient over top ring

Δt = time step

σ = standard deviation of combined roughness

ϕ_x = pressure flow factor

ϕ_s = shear flow factor

ψ = discharge coefficient

β = mass transfer number

η = oil viscosity

κ = isentropic exponent, air

Literature

[1] Abschlußbericht zum FVV Vorhaben **Ringbewegung**, Forschungsstelle Prof. Woschni, TU München, 1987

[2] Orthaber, G.C.: **Berechnungsverfahren für Oelverbrauch und Blow-By zwischen Kolben, Kolbenringen und Zylinderlaufbuchse**, Dissertation, Graz, 1992

[3] Burnett, P.J.; Bull, B.; Wetton, R.J.: **Characterisation of the Ring Pack Lubricant and its Enviroment,** IMechE Paper TRCP.3494R, London, 1993

[4] Furuhama, S.; Tada, T.: **On the Flow of Gas Through the Piston-Rings (2nd Report, The Character of Gas Leckage)**, Bulletin of JSME, Vol. 4, No. 16, 1961

[5] Ting, L.L.; Mayer, J.E.: **Piston Ring Lubrication and Cylinder Bore Wear Analyses, Part II – Theory Verification**, Trans. of ASME, April 1974

[6] Furuhama, S.; Hiruma, M.; Enemoto, Y.: **Effect of Enlarged Topland Clearance on LOC**, Bulletin of JSME, Vol.29, No.254, 1986

[7] Patir, N.; Cheng, H.S.: **An Average Flow Model for Determining Effects of Three-Dimensional Roughness on Partial Hydrodynamic Lubrication**, Journal of Lubrication Technology, Trans. of ASME, Vol. 100, 1978

[8] Patir, N.; Cheng, H.S.: **Application of Average Flow Model to Lubrication Between Rough Sliding Surfaces**, Journal of Lubrication Technology, Trans. of ASME, Vol. 101, 1979

[9] Kawahara, Y.; Maekawa, K.: **Reduction in Lubricant Oil Consumption of Air-Cooled Gasoline Engines**, Technical Review Vol.28 No.2 (June 91), Mitsubishi Heavy Industries Ltd.

[10] Bartz, W. J.; Wedepohl, E.: **Beeinflussung des Ölverbrauches von Verbrennungsmotoren durch das Motorenöl**, In: MTZ 38 (1977).

[11] Affenzeller. J.: **Schmierspalthöhen und Ölverbrauch bei der Kolbenringschmierung von Verbrennungskraftmaschinen**, Dissertation, Graz, 1973

[12] Jakobs, R.: **Ein Beitrag zum Funktionsverhalten von negativ vertwistenden Minutenringen in der 2. Nut von Fahrzeugdieselmotoren**, Technischer Bericht der GOETZE AG